

# Designing Microfuel Cells for Portable Electronics

**Bas Flipsen**

Department of Industrial Design Engineering,  
Delft University of Technology,  
Landbergstraat 15,  
2628 CE, Delft, The Netherlands  
e-mail: s.f.j.flipsen@tudelft.nl

*The main driving force in the developments of consumer electronics, such as cell phones and laptop computers, is longer run times and more functionality. In this quest for higher energy densities, battery characteristics improve at a constant pace. Fuel cells seem to be the next big technology breakthrough improving energy density with a factor of 3–10 compared with current lithium-ion batteries. In particular, the direct methanol fuel cell (DMFC) is an interesting opportunity because of the high energy capacity of methanol and the handling of the fuel making “charging” easy, safe, and fast. To get information on the different aspects that determine the boundaries of the DMFC power source, a power source for an MP3 player, the Samsung YP-Z5F, is designed. This design is based on a DMFC plus battery (DMFC hybrid) and utilizes standard available components [Flipsen, 2007, “Design Challenges for a Fuel Cell Powered MP3 Player,” International Power Sources Symposium, Bath, Great Britain]. The design of a DMFC hybrid power source in a conventional way (standard practice engineering) will not result in a smaller power source for this particular application. The design has a power and energy densities of lower than the currently available lithium-polymer battery, mainly because of the low fuel-efficiency of the cell at low temperatures, the use of commercially available but still too bulky components, and a large amount of dead space ( $\approx 34\%$ ). There are three ways to increase the power and energy densities of the system. First is by increasing the fuel-efficiency of the cells membrane. Second is by scaling down the system components to the right proportions and third is by improving the systems architecture diminishing empty space. This paper presents the design of a DMFC hybrid with scaled-down components. A literature study is done on the efficiency improvements of DMFC cells. The results are presented in a computer aided design (CAD) model and evaluated, comparing the “improved design” with “standard practice” design and the current lithium-polymer battery. The energy density of the redesigned fuel cell system is still low compared with the used lithium-polymer battery but an improvement to the preliminary design. [DOI: 10.1115/1.4001352]*

## 1 Introduction

In portable products the longing for long run times is one of the driving forces for developments in power sources. At the moment the lithium-ion rechargeable battery is the best option with long run times, low charging periods, and high energy densities of up to  $475 \text{ Wh l}^{-1}$ , increasing with 5–10% every year [1]. According to Ref. [2], the maximum attainable will probably around  $550 \text{ Wh l}^{-1}$ . In the quest for even higher energy density, fuel cells, and especially direct methanol fuel cells (DMFC), seem to be the power source of the future for portable electronics [3].

To test the feasibility of the DMFC system, a design of a fuel cell power-system is made, which can power a flash-drive MP3 player, the Samsung YP-Z5F. A preliminary design is made [4], based on a DMFC plus nickel metal hydrate (NiMH) rechargeable battery, a so-called DMFC hybrid. This design utilizes standard available components. Designing a DMFC hybrid power source in a conventional way (standard practice engineering) does not lead to a smaller power source for this particular application [4]. This is mainly because of the low fuel-efficiency of the cell at low temperatures (303 K), the use of commercially available but still too bulky components, and a large amount of dead space ( $\approx 34\%$ ).

There are three ways to increase the power and energy densities of the system. First is by increasing the fuel-efficiency of the cells membrane. Second is by scaling down the system components to the right proportions and third is by improving the systems archi-

ture diminishing empty space. A new design of a DMFC hybrid is made with the help of a literature study on the efficiency improvements of DMFC cells and by scaling down components. This will lead to advanced characteristics of a fuel cell power-system in consumer electronics and gives guidelines for further research. The results are presented in a CAD model and evaluated, comparing the “improved design” with “standard practice” design and to the current lithium-polymer battery.

## 2 Preliminary Design

In Ref. [4] the application field of DMFC systems is reviewed. A comparison is made between the DMFC and the lithium-ion battery with a so-called volumetric Ragone plot. This plot shows that the DMFC has a very high energy density compared with the lithium-ion battery but also a very low-power density. To research the application field of both power/energy sources, the power and energy characteristics of different consumer electronics have been added to the Ragone plot (Fig. 1) and the three application fields can distinguished as follows:

- A. high power density products ( $>80 \text{ W l}^{-1}$ ) such as the PDA and laptop computer
- B. a field of opportunity for a combination of the lithium-ion battery and the DMFC, the DMFC hybrid
- C. the low-power ( $<55 \text{ W l}^{-1}$ ), long endurance products such as smoke detector and low-power wireless-sensors

Most consumer electronics can be found in field A, meaning, the power density of the power source in question should be high (in between  $80 \text{ W l}^{-1}$  and  $500 \text{ W l}^{-1}$ ). A DMFC system alone cannot meet with this high power density but if the DMFC is

Manuscript received November 10, 2009; final manuscript received November 20, 2009; published online August 25, 2010. Review conducted by Nigel M. Sammes.

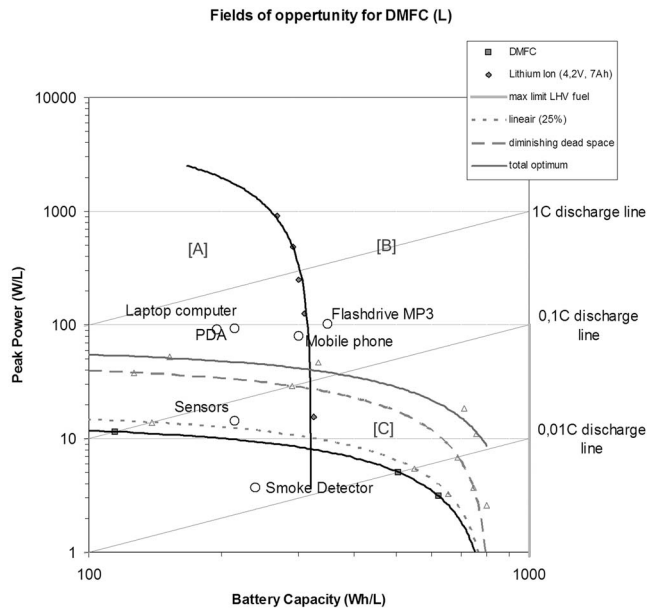


**Fig. 1 Volumetric comparison of the lithium-ion battery and a DMFC power-system**

combined with a battery the endurance of the power/energy source can be extended with a factor of 2–7. The hybrid power-system uses best of both worlds: high energy density of the methanol and high power density of the lithium-ion battery. Because, generally, the runtime of a flash-drive portable MP3 player is high, this product is a good application for hybrid fuel cell systems.

**2.1 Program of Requirements.** The preliminary design of a fuel cell powered MP3 player is based on the following required power output range, runtime user profile and physical limits [4]:

- The power-system plus the fuel-tank has to fit in the battery compartment of the Samsung YP-5Z MP3 player ( $66 \times 33 \times 4 \text{ mm}^3$ ) and has to weigh less than 21 g.

- The system peak power has to be at least 868 mW and maximum of 900 mW.
- The power-system should work for an intensive user, requiring a standardized user profile for at least 2 h or 30 cycles per day.
- The runtime of the power-system should equal or exceed that of the existing lithium-polymer battery (17 h for intensive user, 46.5 h maximum).
- The energy available for an intensive user should be equal to 3.1 Wh.
- The power and energy densities of the system should be equal or exceed  $100 \text{ W l}^{-1}$  and  $348 \text{ Wh l}^{-1}$ .
- The power-system module should be easy to assemble and disassemble.

**2.2 Sizing and Design of the Fuel Cell Power-Source.** In Fig. 2, a functional overview is given for all components, mass flows interconnections, and electronic interconnections. An intermediate accumulator is needed to take care of the peak-power load resulting in a decrease in the fuel cell volume, weight, and system costs.

The design of the system is based on a constant power output of the fuel cell system of 150 mW. Taking charge efficiency, Ohmic losses ( $\approx 90\%$ ), and power using auxiliaries ( $\approx 10\%$ ) into account, the power output of the fuel cells should be around 185 mW. The liquid and gas flows are calculated according to the model described in Ref. [4] and Larminie and Dicks [5]. For a 185 mW output, the flows are described in Table 1. The specifications of the main components are summarized in Table 2 and Fig. 3 [4].

The fuel cell hybrid system designed can power a flash-drive MP3 player. The CAD model of the power-system shows the system cannot fit into the space available in the Samsung MP3 player. The power systems size is  $35 \times 86 \times 8.1 \text{ mm}^3$  (24.4 ml) and the total volume of all main components alone is equal to 16.3 ml. The volume breakdown of the systems space is shown in Fig. 4.

The list of requirements stated that the total volume should not exceed 8.7 ml, at equal specifics. The total amount of energy the designed power-system delivers is equal to that of the used battery, resulting in an energy density of only  $135 \text{ Wh l}^{-1}$  and a

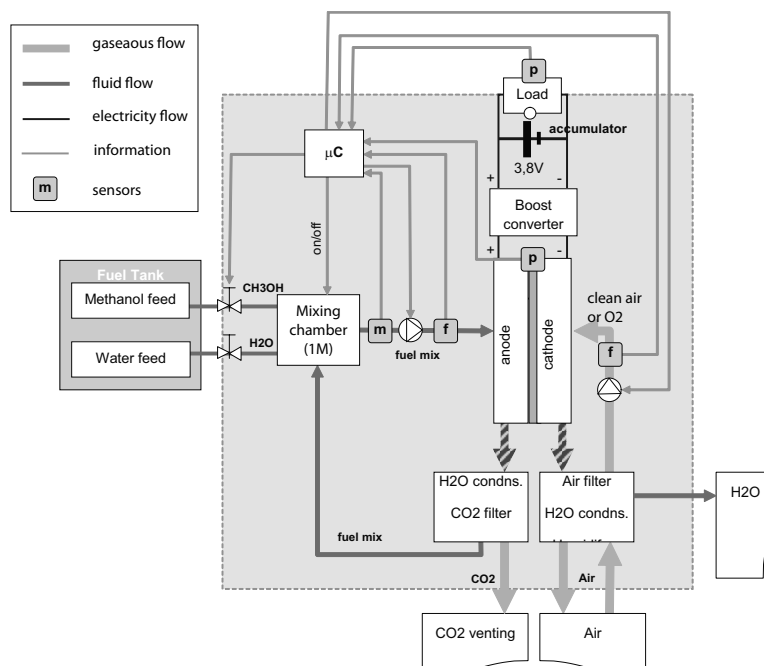


**Fig. 2 Functional overview of all components in the DMFC system**

**Table 1** Calculated in- and outgoing mass flows in the fuel cell power-system producing a constant systems power output of 150 mW [4,5]

Anode in		Anode out	
CH <sub>3</sub> OH	31 $\mu\text{l min}^{-1}$	CH <sub>3</sub> OH	28 $\mu\text{l min}^{-1}$
H <sub>2</sub> O	783 $\mu\text{l min}^{-1}$	H <sub>2</sub> O	766 $\mu\text{l min}^{-1}$
		CO <sub>2</sub>	1679 $\mu\text{l min}^{-1}$
Cathode in		Cathode out	
Air flow of	26.8 ml min <sup>-1</sup>	CH <sub>3</sub> OH x-over	0.6 $\mu\text{l min}^{-1}$
which O <sub>2</sub>	5.07 ml min <sup>-1</sup>	Air flow of which O <sub>2</sub>	24.0 ml min <sup>-1</sup>
			2.54 ml min <sup>-1</sup>
		H <sub>2</sub> O fluid	4 $\mu\text{l min}^{-1}$
		H <sub>2</sub> O vapor	1 $\mu\text{l min}^{-1}$
		H <sub>2</sub> O osmotic	16 $\mu\text{l min}^{-1}$

power density of 37 W l<sup>-1</sup> when taking empty space into account (Table 3). This is almost three times less than the available lithium-polymer battery used in the MP3 player. To decrease volume and increase energy density, the efficiency at low-

**Table 2** Specifications of the main components used in the fuel cell power-system

Component	Type	Specs.	Volume (mm <sup>3</sup> )
Fuel cell membrane	Nafion 117		3 × 14 × 14
Capacitor	2 × Varta V40HR NiMH	1.2 V, 20 m A h	∅11.5 × 5.4
Methanol tank	blow molded	3.3 Wh	4000
Water tank	blow molded	-	4000
Fuel pump	Bartels MP5	0.05–5 ml min <sup>-1</sup>	14 × 14 × 3.5
Air pump	2 × Bartels MP5	0.05–15 ml min <sup>-1</sup>	14 × 14 × 7

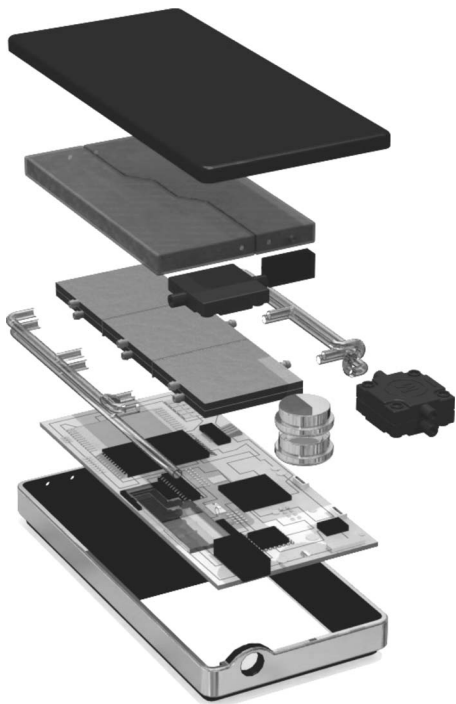


**Fig. 3** Exploded view of the DMFC hybrid, integrated in the MP3 players casing

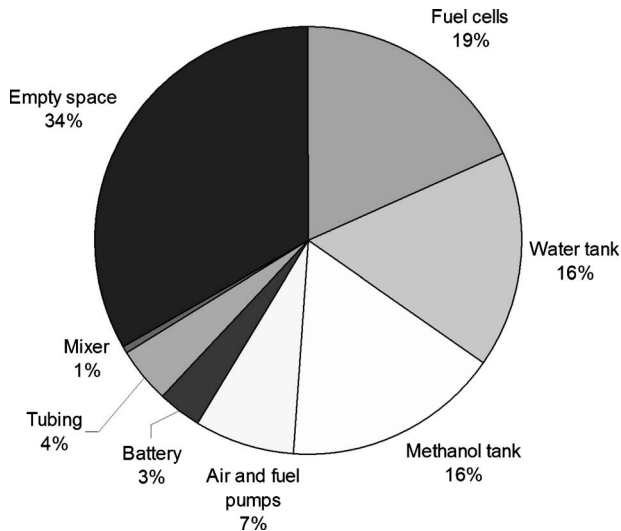


**Fig. 4** Volume breakdown of the fuel cell power-system at a total volume of 24.4 ml

temperature operation (303 K) should be higher, empty space should be diminished, and finally the components should be smaller.

### 3 Redesign of the DMFC Hybrid

The energy density could be increased by increasing the fuel-efficiency and by using scaled-down components. In this section the fuel cell membrane efficiency is compared with state of the art efficiencies described in literature. Higher efficiencies result in a smaller fuel cell flat-pack and less fuel needed. The redesign of the scaled-down fuel cell flat-pack and the resizing of the fuel-tank are described in the following two sections. Sections after will go more into the detail of scaling down the intermediate accumulator, pumps, and other components.

**3.1 Resizing the Fuel Cell Flat-Pack.** The Nafion 117 membrane is normally used in direct methanol fuel cells. The efficiency of the membrane electrode assembly (MEA) is quite high compared with its competitors. The cell performance can generally be characterized with polarization and power curves. In the model for the preliminary design, the membrane is dimensioned for use at a constant nominal load of 185 mW needed to charge/discharge the battery and auxiliaries such as pumps.

Figures 5 and 6 show the polarization and power curves for the cell used in the model. These figures are based on the model described in Ref. [4]. The figures also show other curves taken from recent literature [6–8].

At least three membranes are needed to acquire a workable voltage of 0.761 V. The nominal current is 125 mA cm<sup>-2</sup> and the membrane efficiency in this case is equal to 21%. The operating temperature of the cell is calculated using a thermodynamic model made for the power-system. The final working temperature will

**Table 3** Comparison between the lithium-polymer battery used and the preliminary design of the DMFC hybrid with (i) and without empty space (ii)

		Li-poly battery	DMFC hybrid (i)	DMFC hybrid (ii)
Volume	(ml)	8.7	24.4	16.3
Energy	(Wh)	3.1	3.3	3.3
Energy density	(Wh l <sup>-1</sup> )	348	135	203
Power density	(Wh l <sup>-1</sup> )	103	37	55

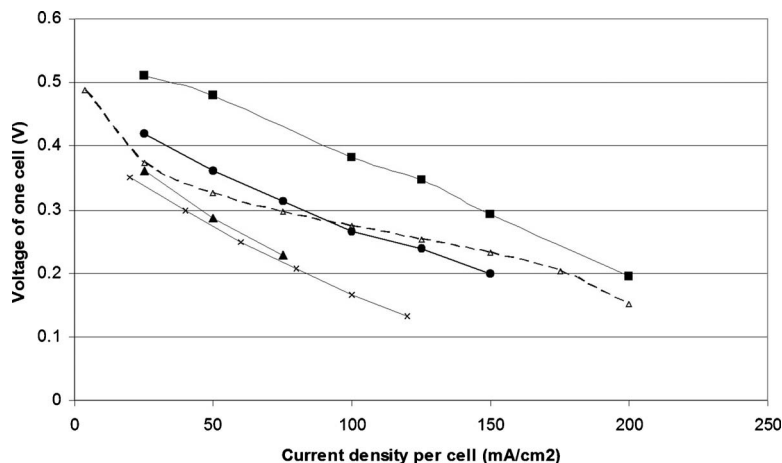


Fig. 5 Polarization curves of Nafion 117 MEAs found in literature [6–8] plus the analytical model (dashed line) [4]

not exceed 303 K. Most curves found in literature are based on high temperature operation (333–353K) while the temperature of the microscale fuel cell will probably not be more than 310K. Temperature has a great influence on the performance of the cell. Different polarization and power curves are found in recent literature [6–8], shown in Figs. 5 and 6. Besides the direction of the polarization curve, the modeled polarization curve fits the current measured low-temperature curves from literature quite good. Probably, the Ohmic losses are higher in real setups than assumed in the model.

The cell developed by Padhy and Reddy [7] had a slightly better performance curve than our model. The efficiency of the cell is slightly better. At a nominal current density of  $125 \text{ mA cm}^{-2}$  the Padhy cell has an efficiency of 29% instead of 21% for the model. The improved performance of the Padhy cell is mainly due to more efficient SS316 endplates with modified serpentine flow field. Assuming this efficiency can be met in the renewed design the active area of one cell could be decreased from  $1.4 \times 1.4 \text{ cm}^2$  to  $1.2 \times 1.2 \text{ cm}^2$ .

**3.2 Resizing the Fuel Tanks.** The previously described efficiency increase also influences the amount of fuel needed to comply with the demand. The volume of the methanol tanks will decrease with a factor of 1.4 compared with the preliminary design. In the new design, only 2.7 ml of methanol and 1 ml of water is consumed to fulfill the requirement of 3.1 Wh of energy. Again it is assumed that the water produced by the cell is recycled as much as possible. For the final redesign the water tank is as large as the methanol tank, both with a storage volume of 2.79 l ( $\approx 3.17 \text{ Wh}$ ).

**3.3 Resizing the Intermediate Accumulator and Trends for the Future.** Commercially available rechargeable button cells, as used in the preliminary design, are mainly produced for application in low-power backup power for personal-computer real-time clocks and BIOS configuration data. The low discharge characteristics make them not very useful for application in the fuel cell battery hybrid design. In general the battery used in the preliminary design is used as a peak-power generator. Per cycle the bat-

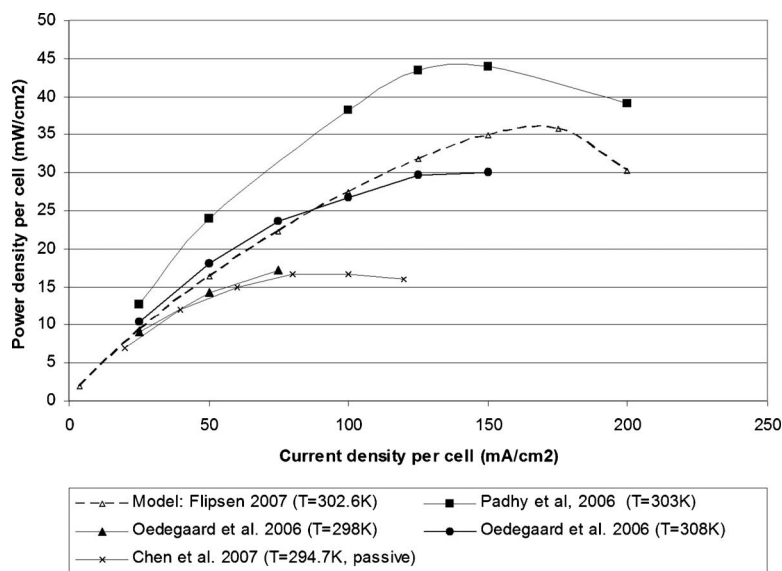


Fig. 6 Power curves of Nafion 117 MEAs found in literature [6–8] plus the analytical model (dashed line) [4]

**Table 4 Overview of commercially available supercapacitors and two prototypes, taken from Refs. [9–11]**

	Voltage (V)	C (F)	Energy (Wh)	Weight (kg)	Volume (l)	Spec. E (Wh kg <sup>-1</sup> )	Spec. P (Wh kg <sup>-1</sup> )	E. density (Wh l <sup>-1</sup> )	P. density (Wh l <sup>-1</sup> )
Maxwell	2.7	350	0.26	0.06	0.05	4.4	1068	5.28	1282
Maxwell PC10	2.5	10	0.009	0.0063	0.0034	1.37	660	2.57	1240
Maxwell PC5	2.5	4	0.003	0.004	0.0016	0.84	470	2.13	1185
Ness	2.7	1800	1.35	0.38	0.277	3.6	975	4.94	1338
Asahi glass	2.7	1375	1.03	0.21	0.151	4.9	390	6.81	542
Panasonic	2.5	1200	0.77	0.34	0.245	2.3	514	3.19	713
Power syst.	2.7	1350	1.01	0.21	0.15	4.9	650	6.86	910
Fuji Heavy Ind. hybrid	3.8	1800	2.67	0.232	0.143	9.2	1025	14.93	1663
A power cap	2.7	55	0.04	0.008	0.006	5.0	8300	7.0	11,620
Skeleton	2.7	1422	1.07	0.201	0.137	5.3	2929	7.8	4311

tery discharges within 1 min and is charged in 3 min. This 4 min charge/discharge-profile of the battery demands the following for the battery used [4]:

1. high discharge rate up to 60 C
2. high charge rate up to 20 C
3. long cycle life more than 16,000 cycles

The demands above cannot be met with commercially available rechargeable button cells. This is mainly because of the low rated (dis)charge rate of rechargeable button cells and their low cycle life of 1000 cycles. By taking a larger cell the charge and discharge rate will decrease but this also results in a larger and bulky battery. In the preliminary design, two Varta V40HR NiMH button cells were used, which could comply with the charge and discharge demands and still be small. For the chosen load-profile all rechargeable batteries will reach their expected maximum number of cycles at 1000 cycles (10% DOD), meaning in this case after 3 months. The alternatives are either using another intermediate accumulator, such as a capacitor, or changing the load-profile of the battery to a longer cycle period. Alternative accumulators are high capacity capacitors, or electric/electrochemical double layer capacitors (EDLCs). The electrochemical DLC is also designated as supercapacitor, ultracapacitor, or pseudocapacitor and is a unique electrical storage device, which can store more energy than conventional capacitors and offer high power density [12]. Most commercially available electrochemical DLCs have a low specific energy below 10 Wh kg<sup>-1</sup> compared with rechargeable batteries.

In Table 4, an overview is given of commercially available supercapacitors and two prototypes. Most of the supercapacitors are very voluminous because of the interesting application field of hybrid and electric vehicles (0.05–0.547 l). The smallest in size is 0.0016 l (Maxwell PC5) and has an energy density of 2.13 Wh l<sup>-1</sup>.

Most developments are directed to increasing the specific energy as can be seen in the prototype carbon/carbon devices in Table 4. The specific energy is projected to increase from 4 Wh kg<sup>-1</sup> to 5 Wh kg<sup>-1</sup> [9]. For our design, we are interested in the energy density (per unit of volume) instead of the specific energy (per unit of mass). To compete with the NiMH batteries chosen in the preliminary design, the supercapacitor has to have an energy density of at least 9.3 Wh l<sup>-1</sup>. As shown in Table 4, all commercially available supercapacitors have an energy density lower than 7 but for the power-system (2.7 V) and the Fuji Heavy Industry Hybrid (3.8 V). According to the press releases in 2005 [11], Fuji even prototyped a li-ion hybrid capacitor with energy density boosted up to 27 Wh l<sup>-1</sup>. This capacitor uses li-ion battery electrodes.

Applying high energy dense supercapacitors in our application will not only decrease volume but also solve the problem of cycle life. According to Burke [9], it is unlikely that capacitors “using battery-like electrodes will have a cycle life comparable to the carbon/carbon devices (greater than 500,000 cycles) for deep dis-

charges. However, a cycle life of 100,000 deep cycles seems possible by proper design of the battery-like electrode.” For our application, this maximum number of deep cycles is sufficient.

In Ref. [4], a preliminary comparison is made among Varta V40HR NiMH battery, Varta MC621 li-ion battery, and Maxwell PC10 supercapacitor. The PC10 capacitor has an energy density of 2.57 Wh l<sup>-1</sup> (capacity of 8.6 m Wh) and is more bulky than two NiMH button cells from Varta. When the Fuji Heavy Industry hybrid capacitor is scaled-down to the required energy demands (10.6 m Wh), a capacitor with a volume of 710 mm<sup>3</sup> is feasible. Based on the form of the PC10 the capacitor could have the following dimensions:

$$h \times w \times d = 13.6 \times 10.8 \times 4.8 \text{ mm}^3$$

**3.4 Liquid Pump.** The fuel pump chosen in the preliminary design was a Bartels MP5 micropump [13]. When the fuel cells have to deliver a constant power of 185 mW, the fuel flow should be 814  $\mu\text{l min}^{-1}$  (Table 1). The maximum liquid flow of the Bartels MP5 pump is in between 4.5 ml min<sup>-1</sup> and 5 ml min<sup>-1</sup> [13]. The liquid flow needed is less than 1 ml min<sup>-1</sup> meaning the used component is a factor 5.5 times to powerful.

In Vishal et al. [20] and Laser and Santiago [21], an overview is given of different techniques to pump small amounts of liquids. In general, the micropumps considered in literature are classified in mechanical pumps, such as rotary and vibrating diaphragm pumps, electrokinetic micropumps, magnetokinetic micropumps, phase change micropumps, and other novel techniques.

In Ref. [21], the term self-pumping frequency  $f_{sp}$  is introduced, which is an interesting metric ratio of maximum flow rate to the package size.

$$f_{sp} = \frac{Q_{\max}}{\text{Vol}} \quad (1)$$

If we compare piezoelectromechanical diaphragm pumps to electromagnetic micropumps the self-pumping frequency of the latter is much lower. For both commercially and laboratory pumps, the volume of the electromagnetic pump is a factor 3–7 larger than the piezoactuated pump (Table 5). When volume is of great importance, such as in the design of the microfuel cell system described, piezoactuated diaphragm pumps seem to be more interesting. Reviewing other pumps under development, such the electrohydrodynamic (EHD) and electroosmotic pump, a big improvement in minimizing the pumps volume is achievable.

For middle long period, the piezodiaphragm pump will be the right choice. At the Fraunhofer Institut IZM a lot of development is going on in the field of piezoactuated diaphragm micropumps [22–24]. In Table 6, an overview is given of the micropumps developed in the laboratories of Fraunhofer Institut IZM. From personal communication with Dr. Richter [25], it became clear that the high flow pump is being industrialized. The self-pumping ratio

**Table 5 Overview of different commercially and laboratory micropumps [13–19]**

Company	Type	Year	Availability	Pump technique	Volume (mm <sup>3</sup> )	Max liquid flow (μl min <sup>-1</sup> )	SPR (min <sup>-1</sup> )	Power ratio (mW min l <sup>-1</sup> )
			Com./Lab.	Actuator				
Bartels	MP5	2006	C	Diaphragm, piezo	686	5000	7.3	40
ThinXXs	MDP1304	2007	C	Diaphragm, piezo	1383	7000	5.1	33
Schwarzer	SP V 125 PZ-L	2009	C	Diaphragm, piezo	20,535	30,000	14.6	1.7
Böhm et al.	-	1999	L	Diaphragm, piezo	288	1900	6.6	-
Böhm et al.	-	1999	L	Diaphragm, EM	1000	2100	2.1	0.24
HNP	MZR-2521	2006	C	Annular gear, EM	9955	9000	0.9	333
Richter et al.	-	1991	L	EHD, injection	6.84	14,000	2047	-
Chen et al.	-	2000	L	ElectroOsmotic	0.003	15	4386	1.4

of these micropumps is a factor of 5–10 higher than the commercially available pumps.

When miniaturizing piezopumps to the volume flow of need scale, effects have to be taken into account. The self-pumping frequency of the two commercially available piezopumps are 5.1 to 7.3 with a mean of 6.3 (Table 5).

For the liquid pump needed in our design this means the pump should be a factor 5.5 smaller than the chosen Bartels MP5 micropump in the preliminary design. This results in a volume of approximately 125 mm<sup>3</sup>. The Bartels pump dimensions are equal to 3.5 × 14 × 14 mm<sup>3</sup>. Because the deflection of the piezoelement will decrease with decreasing width and depth, scaling will be equal in all three directions resulting in a pump with the following dimensions:

$$h \times w \times d = 2.0 \times 7.9 \times 7.9 \text{ mm}^3$$

If we take the developments of IZM into account, the fuel pump could even be an extra factor 5–10 smaller, resulting in pump dimensions of 12.5–25 mm<sup>3</sup>. Take in mind the pump dimensions published by Fraunhofer are without connectors and housing.

**3.5 Air Pump.** When the fuel cells have to deliver a constant power of 185 mW the airflow should be 26.8 ml min<sup>-1</sup> (Table 1). The maximum airflow of an MP5 pump is 15 ml min<sup>-1</sup> so at least two pumps were needed to fulfill the required flow. In the preliminary design two Bartels MP5 pumps were used. At the time of designing the fuel cell system in 2007 [4], Bartels announced the MP6, combining two piezoactuators inside one single housing and a maximum gas flow of 20 ml min<sup>-1</sup> [13], stored in a housing of 30 × 15 × 3.8(1710) mm<sup>3</sup>.

The alternatives for piezoactuated air pump are passive airflow or a rotating electromagnetic actuated flow generator. In Table 7, an overview is given of different air pumps.

For passive airflow the output characteristics will fluctuate, meaning, the desired airflow is not always met. Because of constant airflow, this option is left out and an actuator is used to force the air in the cells.

Based on Table 7 electromagnetic and electrostatic diaphragm pumps seem to be less bulky for the function of delivering airflow, as shown by the self-pumping ratio. Thus, the two Bartels MP5

**Table 6 Overview of new developments in micropumps from Fraunhofer Institut IZM [3,22,23]**

Company	Type	Year	Availability	Pump technique	Volume (mm <sup>3</sup> )	Max liquid flow (μl min <sup>-1</sup> )	SPR (min <sup>-1</sup> )	Power ratio (mW min l <sup>-1</sup> )
			Com./Lab.	Actuator				
Richter	Standard	2007	L	Diaphragm, piezo	54	2000	38	-
	High flow	2009	L	Diaphragm, piezo	54	4000	74.1	-
	High pressure	2009	L	Diaphragm, piezo	54	400	7.4	-
	Micro	2009	L	Diaphragm, piezo	18	1000	55.6	25
	High perform.	2009	L	Diaphragm, piezo	2827	12,000	4.2	-

**Table 7 Overview of gas flow pumps [13,14,16,25–30]**

Company	Type	Year	Availability	Pump technique	Volume (mm <sup>3</sup> )	Max gas flow (μl min <sup>-1</sup> )	SPR (min <sup>-1</sup> )	Power ratio (mW min l <sup>-1</sup> )
			Com./Lab.	Actuator				
Kaemper et al.	-	1998	L	Diaphragm, piezo	504	3500	6.9	-
Cabuz et al.	-	2001	L	Diaphragm, piezo	225	30,000	133.3	2.67 × 10 <sup>-4</sup>
Bartels	MP5	2006	C	Diaphragm, piezo	686	15,000	21.9	0.013
	MP6	2008	C	Diaphragm, piezo	1710	20,000	11.7	0.010
ThinXXs	MDP1304	2007	C	Diaphragm, piezo	1383	22,000	15.9	0.046
Schabmueller	-	2002	L	Diaphragm, piezo	120	690	5.8	-
Richter	Standard	2007	L	Diaphragm, piezo	54	10,000	185	-
	High flow	2009	L	Diaphragm, piezo	54	40,000	740	-
	High pressure	2009	L	Diaphragm, piezo	54	1000	18.5	-
	Micro	2009	L	Diaphragm, piezo	18	4000	222	-
	High performance	2009	L	Diaphragm, piezo	2827	35,000	124	-
Böhm et al. [16]	-	1999	L	Diaphragm, EM	1000	40,000	40.0	-
Xavitech	V200-GAS	2008	C	Diaphragm, EM	16,300	450,000	27.6	0.005
Thomas	BL-G 085 M	2006	C	Rotary vane, EM	50,000	8.5 × 10 <sup>6</sup>	172.2	2.8

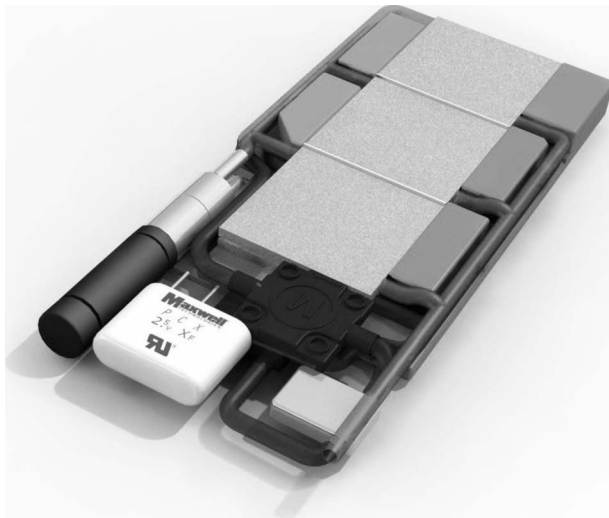


Fig. 7 The fuel cell power-system assembly

pumps are replaced by an electromagnetic diaphragm pump with dimensions based on a  $f_{sp}$  of 34. The pump dimensions will be almost 40% smaller, 883 mm<sup>3</sup>, than the two Bartels MP5 pumps put together. Electromagnetic actuated pumps are mostly not flat designs but more long and cylindrical.

$$l \times \frac{1}{4} \pi d^2 = 31 \times \frac{1}{4} \pi \cdot 6^2 \text{ mm}^3$$

Based on the pumps developed by Fraunhofer Institut IZM, the self-pumping ratio could even be an extra factor 10 higher. Again, it has to be taken into account that all data of the laboratory pumps is without casing ( $\approx 60\%$  of total volume).

**3.6 Other Components: Tubing and Electronics.** Besides the previously mentioned components air and fuel has to be delivered to the fuel cells. Flexible tubing is used with an outer diameter of  $\varnothing 2$  mm. The tubes have a limited bending ratio, which has to be taken into account. Two tanks are needed to fuel the DMFC system, one filled with water and one with methanol. A small passive mixer will mix the water and methanol to the right concentration (3% w/w). The mixture will be controlled by two valves. A small methanol microsensors will measure the concentration after the mixing tank, controlling the valves. The microsensors are under development by Integrated Sensing Systems, Inc. (IS-SYS) and Kyoto electronics Manufacturing company (KEM), and an estimate of the dimensions is made based on published data [31].

**3.7 Assembly of the Improved Design.** In Fig. 7, the final assembly of the fuel cell power-system is shown. All components are modeled excluding the electronic interconnections. In this design, it is assumed the controllers are integrated on the printed circuit board (PCB) of the MP3 player. The specifications of the main components are summarized in Table 8.

#### 4 Conclusions and Recommendations

A redesign of the 185 mW microfuel cell power-system has been made. The fuel cell hybrid system can power a flash-drive MP3 player. The redesign is based on components scaled-down to fit the specifics needed for powering the application. A CAD model has been made to show the feasibility of the redesign as a replacement for a lithium-ion battery. The power systems size is 83.2 × 36.0 × 6 mm<sup>3</sup> (18.0 ml) and the total volume of the main components alone is 14.0 ml (Fig. 8). In the preliminary design, the fuel tanks were designed as a box. In the redesign the tanks are formed fitting in between the tubing and acting as a platform were

Table 8 Specifications of the main components used in the redesigned fuel cell power-system

Component	Type	Specs	Volume (mm <sup>3</sup> )
Fuel cell membrane	3 × Nafion 117	0.53 V <sub>OC</sub>	3 × 14 × 14
Capacitor	Supercapacitor	10.6 m Wh	13.6 × 10.8 × 4.8
Methanol tank	Blow molded methanol	t=0.25 mm	3570
		3.17 Wh	2790
Water tank	Blow molded	-	3570
Fuel pump	Piezo diaphragm.	-	7.9 × 7.9 × 2.0
Air pump	Electromagnetic	-	31 × $\varnothing 6$

all components can be fitted on. This gives two advantages over the preliminary design: (i) more empty space is used and (ii) during assembly the components can be fitted to the tanks, making the subassembly easier to handle.

In Fig. 9, the volume breakdown of the system space is shown. The system still does not fit in the compartment available for the battery.

The list of requirements stated that the total volume should not exceed 8.7 ml, at equal specifics. The designed DMFC hybrid exceeds this volume with almost 10 ml. In Table 8 the specifics of the design are shown. The energy contained in the system is 3.17 Wh making the energy density of the system equal to 176 Wh l<sup>-1</sup>. In Table 9 the redesign is compared with the preliminary design and with the lithium-polymer battery.

The energy density is high compared with the preliminary design but still very low compared with the lithium-polymer battery. This is because of the large amount of water (20%), the large volume taken in by the fuel cells (20%) and the empty space in the system (22%).

The system only uses 1 ml of water effectively but an extra 1.79 ml is added for losses in the system. The amount of water contained could be decreased when all water in the system is recycled into the system. An improvement of 1.79 ml is feasible.

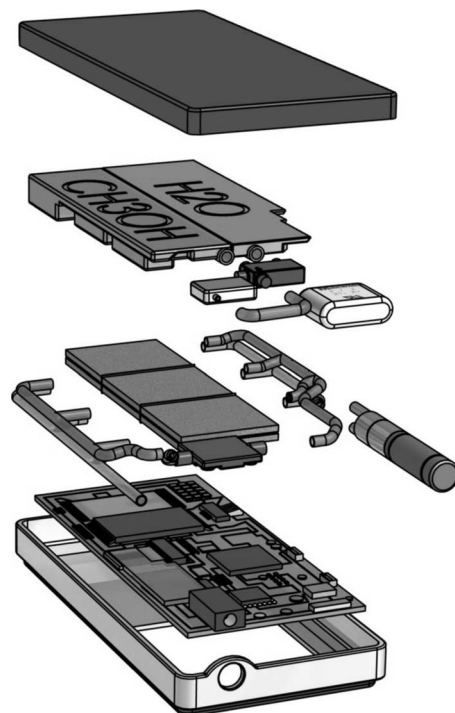
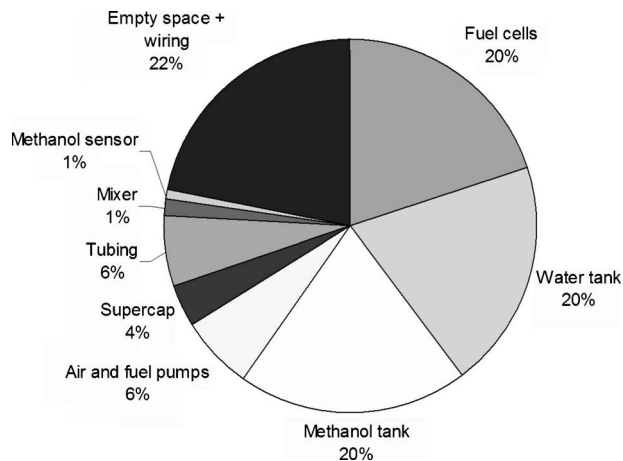


Fig. 8 Exploded view of the fuel cell power-system assembly



**Fig. 9** Volume breakdown of the redesign of the fuel cell power-system (total volume of 18.0 ml)

**Table 9** Comparison among the lithium-polymer battery, the preliminary design, and the redesign

	Lithium polymer battery	Preliminary design	Redesigned DMFC hybrid
Volume (ml)	8.7	24.4	18.0
Component (ml)	-	16.3	14.0
Dimensions (mm)	66 × 33 × 4	86 × 35 × 8	83 × 36 × 6
Energy (Wh)	3.1	3.3	3.17
E. density (Wh l <sup>-1</sup> )	348	135/202	176/226
P. density (Wh l <sup>-1</sup> )	103	37.55	50/64

Another option is using fuel cells, which work on higher concentration or even pure methanol such as the one presented in 2005 by Toshiba [32]. In 2008, Toshiba presented new developments at the CEATEC 2008 in Japan.

Because of stiffness requirements, the end plates on the flat-pack cells have a thickness of 1.5 mm. At least 0.5 mm of the thickness of one plate is needed for the serpentine flow field. The thickness could be decreased to probably 1 mm making the total volume decrease with 1.1 ml. Another option is to use a stacked design instead of a flat-pack design. The two bipolar plates needed in the stacked design could have a thickness of 0.5–1.0 mm. The thickness of the total system, although, will increase to 4–5 mm.

The fuel cell efficiency at low-temperature (303 K) of the cells used is high (29%). Improving low-temperature efficiency of the cells will decrease system volume severely, mainly because of the decrease in the cell volume and the amount of fuel and water needed.

The amount of empty space is still high in this redesign (22%) but almost halved compared with the preliminary design. Using the tank as a filler makes the use of the volume available more efficient. More improvements by changing the architecture of the system are still feasible.

An other option to decrease volume is by improving load-balancing of the DMFC and the battery. Changing the “operational strategy” can have influence on the total volume of the system. In a follow-up research project, the influence of operational strategy on the energy density will be investigated.

## Acknowledgment

The author would like to thank Maarten Kamphuis for making the CAD model and the final renderings of the fuel cell power-system. Furthermore, special thanks to my colleague Ruben Strijk and Katrijn Coninx for their support in the fuel cell model and for the calculations and review of the paper.

## References

- [1] M. Rynänen, M., and Tasa, S., 2005, Optimized Energy for Future Mobile Multimedia Devices.
- [2] Broussely, M., and Archdale, G., 2004, “Li-Ion Batteries and Portable Power Source Prospects for the Next 5–10 Years,” *J. Power Sources*, **136**(2), pp. 386–394.
- [3] Flipsen, B., 2006, “Power Sources Compared: The Ultimate Truth?,” *J. Power Sources*, **162**(2), pp. 927–934.
- [4] Flipsen, B., 2007, “Design Challenges for a Fuel Cell Powered MP3 Player,” International Power Sources Symposium, Bath, Great Britain.
- [5] Larminie, J., and Dicks, A., 2003, *Fuel Cell Systems Explained*, Wiley, Chichester.
- [6] Oedegaard, A., and Hentschel, C., 2006, “Characterisation of a Portable DMFC Stack and a Methanol-Feeding Concept,” *J. Power Sources*, **158**(1), pp. 177–187.
- [7] Padhy, B. R., and Reddy, R. G., 2006, “Performance of DMFC With SS 316 Bipolar/End Plates,” *J. Power Sources*, **153**(1), pp. 125–129.
- [8] Chen, C., Liu, D., Huang, C., and Chang, C., 2007, “Portable DMFC System With Methanol Sensor-Less Control,” *J. Power Sources*, **167**(2), pp. 442–449.
- [9] Burke, A., 2007, “R&D Considerations for the Performance and Application of Electrochemical Capacitors,” *Electrochim. Acta*, **53**(3), pp. 1083–1091.
- [10] Maxwell Technologies, 2004, “Electric Double Layer Capacitor: BOOSTCAP Ultra-Capacitor,” Document No. 1003996, Rev. 6.
- [11] Yোগmogita, H., 2005, “Electrical Storage Technology Combines Li-Ion Capacitors,” *Nikkei Electronics Asia Volume*.
- [12] Jayalakshmi, M., and Balasubramanian, K., 2008, “Simple Capacitors to Supercapacitors—An Overview,” *Int. J. Electrochem. Sci.*, **3**(11), pp. 1196–1217.
- [13] Bartels Mikrotechnik GmbH, 2008, [www.bartels-mikrotechnik.de](http://www.bartels-mikrotechnik.de), Datasheet of the MP5 and MP6 Micropump, URL [www.bartels-mikrotechnik.de](http://www.bartels-mikrotechnik.de).
- [14] ThinXXS Microtechnology AG, [www.thinxxs.com](http://www.thinxxs.com), 2006, Datasheet MDP1304, Micro Diaphragm Pump, URL [www.thinxxs.com](http://www.thinxxs.com).
- [15] Schwartzer GmbH, 2009, SP V 125 PZ-L Datasheet, The Revolutionary Generation of Piezo-Pumps, URL [www.schwartzert.com](http://www.schwartzert.com).
- [16] Böhm, S., Olthuis, W., and Bergveld, P., 1999, “A Plastic Micropump Constructed With Conventional Techniques and Materials,” *Sens. Actuators, A*, **77**, pp. 223–228.
- [17] HNP Mikrosysteme GmbH, 2006, [www.hnp-mikrosysteme.de](http://www.hnp-mikrosysteme.de), Micro Annular Gear Pump MZR(R)-2521 in Dosing Pump for Analytical Instrumentation, URL [www.hnp-mikrosysteme.de](http://www.hnp-mikrosysteme.de).
- [18] Richter, A., Plettner, A., Hofmann, K., and Sandmaier, H., 1991, “A Micro-machined Electrohydrodynamic (EHD) Pump,” *Sens. Actuators, A*, **29**, pp. 159–168.
- [19] Chen, C., Zeng, S., Mikkelsen, J., and Santiago, J., 2000, “Development of a Planar Electrokinetic Micropump,” ASME International Mechanical Engineering Congress and Exposition, Orlando, FL, pp. 523–528.
- [20] Vishal, S., Suresh, V., and Arvind, R., 2004, “Microscale Pumping Technologies for Microchannel Cooling Systems,” *Appl. Mech. Rev.*, **57**, pp. 191–221.
- [21] Laser, D., and Santiago, J., 2004, “A Review of Micropumps,” *J. Micromech. Microeng.*, **14**(6), pp. R35–R64.
- [22] Richter, M., 2006, “Micropumps—From the Lab to the Fab,” *Actuator 2006*.
- [23] Richter, M., 2007, Ersterpreis für die kleinste siliziumpumpe der welt.
- [24] Zhu, M., Kirby, P., Wacklerle, M., Herz, M., and Richter, M., 2009, “Optimization Design of Multi-Material Micropump Using Finite Element Method,” *Sens. Actuators, A*, **149**(1), pp. 130–135.
- [25] Flipsen, B., 2009, Private Communication With M. Richter (fraunhofer institut) About Fraunhofers Micropump.
- [26] Kaemper, K., Doepfer, J., Erhrfeld, W., and Oberbeck, S., 1998, “A Self-Filling Low-Cost Membrane Micropump,” *IEEE, Heidelberg, Germany*.
- [27] Cabuz, C., Herb, W., Cabuz, E., and Lu, S., 2001, “The Dual Diaphragm Pump,” *Micro Electro Mechanical Systems (MEMS)*, IEEE, New York.
- [28] Schabmueller, C. G. J., 2002, “Self-Alignment Gas/Liquid Micropump,” *J. Micromech. Microeng.*, **12**, pp. 420–424.
- [29] Xavitech, AB, 2007, [www.xavitech.com](http://www.xavitech.com), Datasheet: V200 and P200 GAS, URL [www.xavitech.com](http://www.xavitech.com).
- [30] Gardner Denver Thomas, 2006, [www.rtpumps.com](http://www.rtpumps.com), Rotary Vane Pump BL-G 085 M, URL [www.rtpumps.com](http://www.rtpumps.com).
- [31] Sparks, D., Laroche, C., Tran, N., Goetzinger, D., Najafi, N., Kawaguchi, K., and Yasuda, M., 2005, “A New Methanol Concentration Microsensor for Improved DMFC Performance,” *Fuel Cell Summit 2005*.
- [32] Toshiba, 2005, “Toshiba Integrates Prototypes of World’s Smallest Direct Methanol Fuel Cell Unit Into Mobile Audio Players,” Press Release.